# Design methodology of an electric vehicle hybrid energy storage unit for improved energy efficiency

Sébastien Mariéthoz
Automatic Control Laboratory, ETH Zürich
Physikstrasse 3, CH - 8092 Zürich, Switzerland
Email: mariethoz@control.ee.ethz.ch

Philippe Barrade
Laboratoire d'Electronique Industrielle, EPFL
CH - 1015 Lausanne, Switzerland
Email: philippe.barrade@epfl.ch

***Abstract*—This work proposes a design methodology that allows designing the energy storage unit of an electric vehicle in order to minimize the required energy and the resulting losses. A simple analytical model of the vehicle losses is derived. Driving conditions and solar production scenarios are obtained from stochastic processes; they are employed to generate a number of vehicle power profiles. Candidate supercapacitor arrangements are classified in terms of losses and energy capacity, leading to the associated Pareto minimum.**

***Index Terms*—Ultracapacitor, supercapacitor, storage, energy management, electric vehicle, Pareto minimum, loss minimization, stochastic model.**

## I. Introduction

Energy accumulators based on supercapacitors [1], [2] have attracted a lot of interest as solutions to store electrical energy on-board electric vehicles [3]–[5] due to their good robustness, very high power density, high energy density, long life-time and high energy efficiency. They are particularly attractive to support peak shaving in hybrid power systems, where there are several sources of power and storage devices [2], [6].

Design and optimization of energy management systems is complicated by the stochastic nature of the power solicitations that apply to energy storage devices. The model of the stochastic process can be built based on measurement or on the modeling of the stochastic phenomena. The selection of the modeling approach depends on the access to data and on the knowledge of the stochastic phenomena acting on the system. Both approaches have been applied to the design of storage systems [7], [8].

In this work, stochastic models are employed to represent uncertainty in the power production and consumption. The objective is to design an energy management system featuring reduced losses. Several supercapacitor accumulators are designed in order to satisfy the constraints linked to the vehicle autonomy and power electronics system operation. A probabilistic model of driving conditions is elaborated that allows to link the hybrid energy accumulator parameters to the system losses. This allows selecting the more effective accumulator in terms of capacity and energy efficiency. The proposed concepts are applied to a reduced scale electric vehicle (see Fig. 1) that is part of a project initiated at the Automatic Control Laboratory of ETH Zürich in order to teach and investigate topics related to power conversion, energy management and motion control [9].

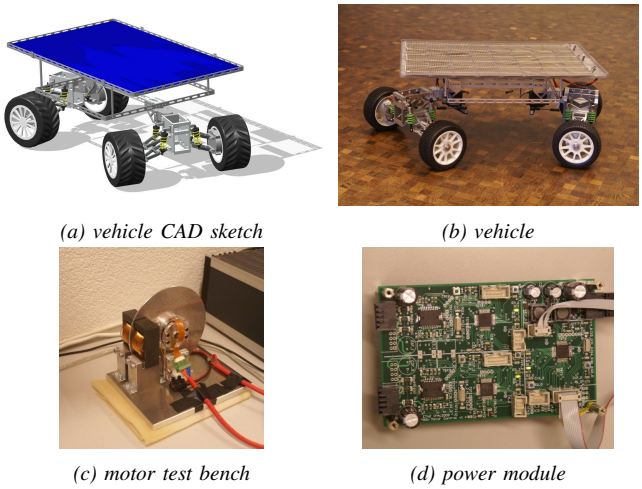

*(a) vehicle CAD sketch* *(b) vehicle*

*(c) motor test bench* *(d) power module*

Fig. 1. Construction stages of the reduced scale electric vehicle and of its energy management system.

## II. Energy management system

The vehicle is driven by two flat 8 pole pairs permanent magnet synchronous motors (PMSM). Its photovoltaic array (see 1(b)) is the primary energy source of the system.

### A. Hybrid accumulator concept

Battery and supercapacitors are combined to build an hybrid accumulator that allows improving system efficiency and life-time. Supercapacitors are smoothing large power fluctuations, while batteries are employed to balance the power on longer time periods.

### B. Power electronics system topology

The energy management system shown in Fig. 2 employs a common DC-bus. The energy management modules connect to this DC-bus through boost converters. The two vehicle drives are directly connected to the DC-bus.

### C. DC-bus voltage control strategy for reduced losses

In order to reduce the system switching losses, the DC-bus voltage is adjusted to fulfill the requirements of the two drive modules, which means the required voltage is approximately

978-1-4244-8218-4/10/$26.00 ©2010 IEEE

proportional to the vehicle speed. The DC-bus voltage cannot however be smaller than the highest of the modules' voltages:

$$u_{\mathrm{bus}} = \max\{u_{\mathrm{pv}}, u_{\mathrm{batt}}, u_{\mathrm{sc}}, u_{\mathrm{mot}}\} \quad (1)$$

(1) means that for high speeds the drives will decide on the bus voltage, while for low-speed the battery voltage level, ultra-capacitor voltage level and incoming irradiance and temperature will be the decision criteria.

## III. Design of the hybrid accumulator and candidate supercapacitor arrangements

In this section, candidate supercapacitor arrangements are identified according to solar power production, power load (or regeneration) and modules' voltage constraints, which impose the power and voltage profiles on the hybrid accumulator. The objective is to ensure vehicle operation in the worst admissible case. The design is therefore based on a worst case model obtained defining the worst slope profile for which the vehicle should be designed and on the solar power production extremes (see worst case driving profile in Fig. 3 and associated worst case power profile in Fig. 4).

### *A. Step 1 – Initial design according to energy and power requirements*

The power and energy profiles that are required for the hybrid accumulator (HA) are derived from the worst admissible case which is defined by:

- A worst case driving profile shown in Fig. 3; this profile is build based on where the vehicle could drive.
- The photovoltaic power profile that causes the maximum power fluctuation given the driving profile. This is obtained from the photovoltaic array dimension, the employed cells' efficiency and the expected irradiance fluctuation. The expected irradiance fluctuation is modeled by a stochastic process.

The resulting power $P_{\mathrm{HA}}$ and energy profiles $W_{\mathrm{HA}}$ are shown in Fig. 4(a).

The hybrid accumulator power is split between the battery and the supercapacitors. The control objective is to minimize the battery energy ripple. The actual power share depends on the implemented control law and precise load cycle. In order to simplify computation, it is assumed that the battery module provides the required constant average power $P_{\mathrm{bat}}$ over the considered profile, while the supercapacitor module provides the power fluctuations. The energy efficiency of the power converter that interfaces the supercapacitors to the DC bus is required in order to determine the power effectively drawn from the supercapacitors after a charge-discharge cycle. This energy efficiency is conservatively assumed to be $\eta_{\mathrm{int,sc}} = 90\%$ after adding/removing converter losses:

$$P_{\mathrm{SC}} = \begin{cases} \eta_{\mathrm{int,sc}}\,(P_{\mathrm{HA}} - P_{\mathrm{bat}}) & P_{\mathrm{HA}} - P_{\mathrm{bat}} > 0 \\ \frac{P_{\mathrm{HA}} - P_{\mathrm{bat}}}{\eta_{\mathrm{int,sc}}} & P_{\mathrm{HA}} - P_{\mathrm{bat}} \leq 0 \end{cases} . \quad (2)$$

The worst case power profile $P_{\mathrm{SC}}$ and energy profile $W_{\mathrm{SC}}$ that are applied to the supercapacitors depicted in Fig. 4(b) are deduced (see the labeled green curves).

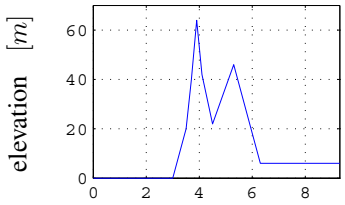


Fig. 3. Worst case driving elevation profile employed for worst case hybrid accumulator design.

TABLE I
Vehicle dimensions.

| | |
|---|---|
| Total vehicle mass | 4.5 kg |
| Weight allocated for hybrid accumulator | 0.6 kg |
| Payload | 2 kg |
| PV array characteristics | 8×6 cells |

Two main criteria deduced from the power and energy profiles must be considered [10] for the supercapacitor tank design:

- Energy requirement: is deduced considering the profile $W_{\mathrm{sc}}$, by measuring the difference $W_{\mathrm{u}}$ between the energy level extrema. Here, $W_{\mathrm{u}} = 1.336\,Wh$,
- Power requirement: is obtained considering the average value of the rectified power profile $P_{\mathrm{sc}}$. Here, $\bar{P}_{\mathrm{sc}} = 5.4\,W$.

Moreover, an additional design constraint is to obtain an efficiency of at least $\eta_{\mathrm{sc}} = 98\%$ for the supercapacitor tank. Considering only the supercapacitors relevant for this application (capacitances ranging from $100F$ up to $350F$), the supercapacitor arrangements fulfilling the requirements defined by the profiles shown in Fig. 4 are shown in Tab. II. From Tab. II, it can be deduced that the supercapacitor tank losses are always smaller than the energy efficiency requirement. There is no need to add any extra supercapacitor cell to fulfil the required efficiency $\eta_{\mathrm{sc}} = 98\%$. This is due to the low series resistor of the considered supercapacitor cells, and to the low power requirements of the considered application. The main sizing criterion is therefore the required energy.

For all considered supercapacitor cells, the final weight is near half of a kilogram, for a volume close to $0.3\,l$. For the considered application, the volume seems not to be the key criterion, while the weight can dramatically increase the vehicle energy consumption (supercapacitor tank is about 10 % of the total weight see Tab. I). If the main criterion is to lower such energy needs, then the tank defined by the lowest weight should be chosen (6 cells $350F$). On the one hand, such a tank is the lightest. On the other hand, it results from a sizing procedure, where the energy requirements are covered with only 40 % voltage discharge. As the maximum voltage discharge can reach 50 %, the supercapacitor tank is clearly over-sized considering only the energy requirements. This oversizing can in turn cover the extra energy needs resulting from the associated weight increase. In this case, it is not necessary to reiterate. If it does not cover these extra needs, one need to readjust the hybrid accumulator parameters

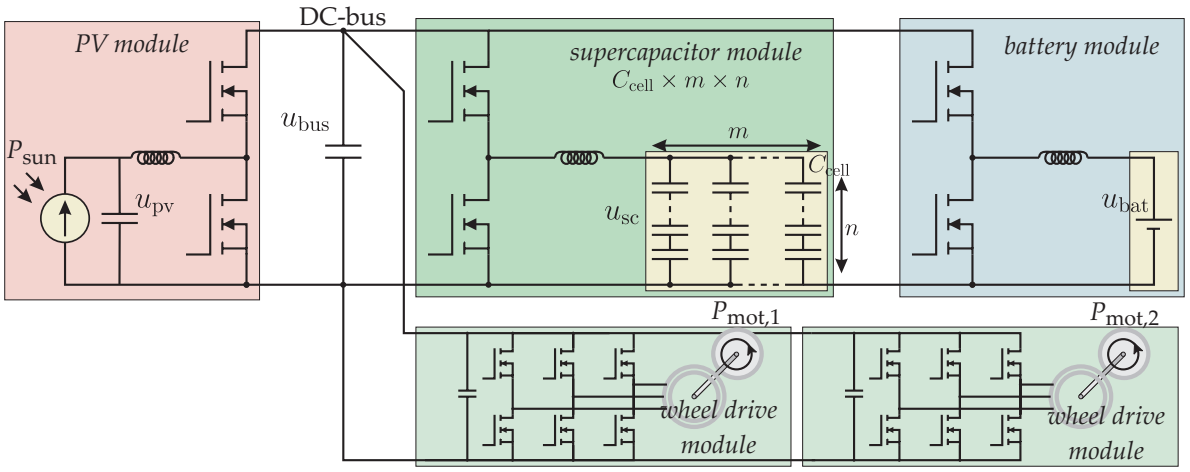


Fig. 2. Considered topology for the motion control and energy management

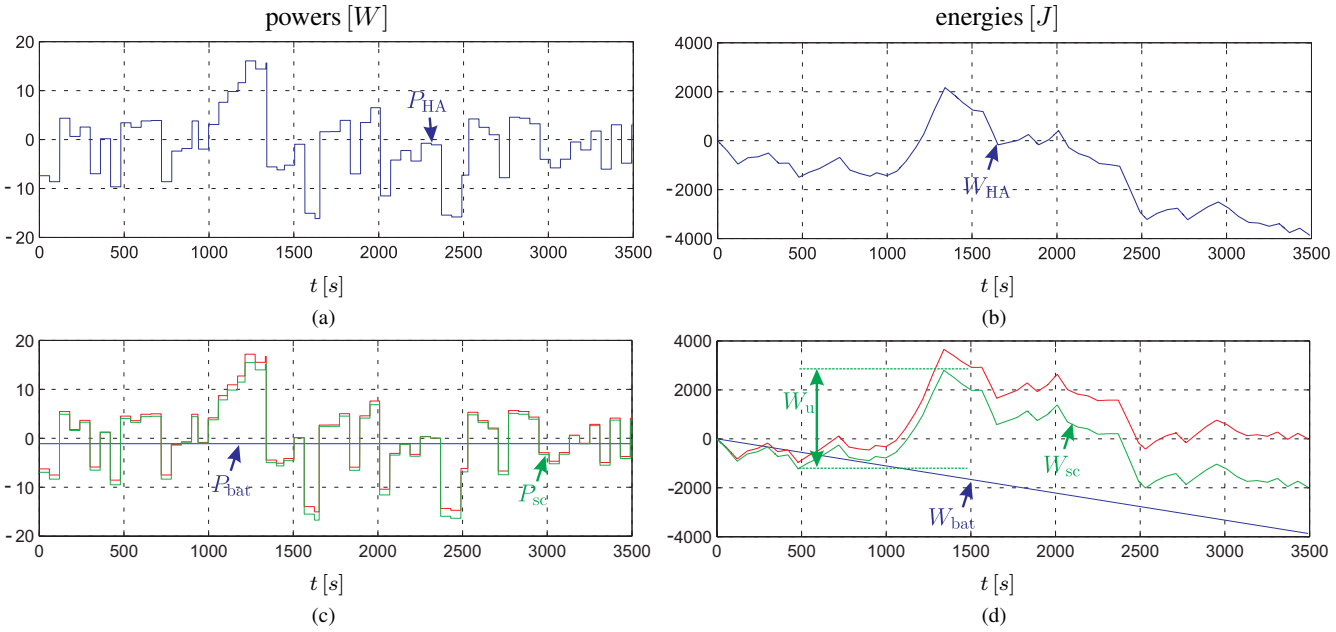


Fig. 4. Power and energy profiles deduced from worst case elevation profile Fig. 3. (a) Corresponding hybrid accumulator solicitation in power; (b) in energy (c) Breakdown between supercapacitors and batteries power; (d) energy

through a design iteration.

### *B. Step 2 – Design taking into account voltage requirements*

In order to complete the supercapacitor tank design, the voltage levels resulting from the supercapacitor series/parallel arrangements have to be considered. The voltage level determines the possible converter topologies that can be employed to interface the accumulator and the vehicle modules and the resulting energy efficiency. For this application the DC bus voltage required at nominal vehicle speed is $u_{\text{bus}} = 35V$. In order to fulfil the topology constraint, and avoid oversizing the supercapacitor arrangement in voltage, the configurations that result in a maximum voltage higher than $u_{\text{sc,max}} = 35V$ are eliminated. The lowest tank charge must be limited in order to ensure that the interface power converter features a sufficiently high energy efficiency: in this case, the lower bound has been fixed to $u_{\text{sc,min}} = 10\,V$. Supercapacitor cells are added to the initial number of supercapacitors $N_1$ obtained in step 1 (see Tab. II) in order to derive a family of supercapacitor arrangements that meet the constraints $10\,V < u_{\text{sc}} < 35V$. The design of the final number of cells is performed following a sequential approach, for all the considered capacitances:

- the initial number $N_1$ of cells from Tab. II is divided in $n$ series connected cells and $m$ branches (see supercapacitor module in Fig. 2), such as $N_1 = n.m$. The supercapacitive tank is then considered as a matrix, whose each elements are the cells. Eventually, $N_1$ is rounded to form a pure rectangular matrix.
- The minimum and the maximum voltage levels of the tank are then checked to identify if they belong to the

TABLE II
SIZING PROCEDURE FOR $P = 5.3996W$ AND $W_u = 1.3368Wh$, DETERMINING SIZING CRITERION: ENERGY

| C [F] | 100 | 150 | 310 | 350 |
|---|---|---|---|---|
| $R_{\mathrm{SC}}$ [Ω] | 0.015 | 0.014 | 0.0022 | 0.0032 |
| $U_{\mathrm{SC}}$ [V] | 2.7 | 2.7 | 2.7 | 2.7 |
| Initial number of supercapacitors: $N_1$ | 18 | 12 | 6 | 6 |
| Minimum charge: $D$ (%) | 51.6 | 51.5 | 53.8 | **60.9** |
| Tank efficiency: $\eta_{\mathrm{sc}}$ | 0.9988 | 0.9984 | **0.9995** | 0.9994 |
| Tank weight (kg) | 0.45 | 0.42 | **0.37** | 0.38 |
| Tank volume (l) | 0.308 | **0.294** | 0.318 | 0.318 |

voltage window $10\,V < u_{\mathrm{sc}} < 35V$. If not, cells are added, and a new pair $(n, m)$ is defined. If yes, different configurations $(n, m)$ are analyzed, and cells are added until the maximum voltage level is exceeded.

It leads to deriving family of candidate solutions that match simultaneously the energy requirements, the power constraints (efficiency) and the voltage constraints. The results are presented in Fig. 5, for the cells initially considered in Tab. II. The voltage variation range is given as a function of the final number of supercapacitors $N_2 = m \cdot n$ (horizontal axis). The arrangements are denoted $m \times n$.

### C. Sizing results' discussion

The arrangements made of the $100\,F$ and $150\,F$ supercapacitor cells directly match the specified voltage variation, without extra cells. However, extra cells can be added if one focuses only on the voltage requirements. In this case ($N_2 > 18$), the tank is oversized regarding the energy and power requirements.

The arrangements made of the $300\,F$ and $350\,F$ lead in any case to the addition of extra cells to match the allowed tank voltage window. The proposed tank sizing leads to a strong over-sizing in energy and power capability, such that the voltage constraints become the only design constraints.

If the priority is given to the lowering of the weight, then $N_2 = 18$ $(100F)$ and $N_2 = 11$ $(150F)$ are the only possible sizing to consider as they match simultaneously energy and voltage requirements without addition of extra cells. For all the other sizing possibilities defined in Fig. 5, the main sizing criterion is linked to voltage levels only, and leads to a non-negligible cell number increase. It impacts then strongly on the weight of the tank. This must be taken into account as a cost function for the choice of the final supercapacitive tank.

In all cases, energy and power requirements are satisfied. It means that the charge/discharge efficiency of the supercapacitive tank will result in an energy efficiency higher than the requested $\eta_{\mathrm{sc}} = 98\%$. As a consequence, the choice of the final supercapacitive tank on efficiency criteria is linked to only to the impact of the supercapacitor voltage fluctuations on the efficiency of the various converters defined in Fig. 2.

## IV. SYSTEM LOSS MODEL

The vehicle energy management and motion control losses are modeled in order to obtain an analytical expression suitable to design the system for minimal losses. In the following analysis, power are identified by the symbol $P$, losses by the symbol $\ell$. The waveform ripples are assumed negligible.

### A. Energy management losses

The energy management losses depend on the DC-bus voltage, power flows and converter parameters. The losses are similar for the supercapacitor module:

$$\ell_{\mathrm{sc}} = |P_{\mathrm{sc}}| \, \frac{u_{\mathrm{bus}}}{u_{\mathrm{sc}}} \, f_{\mathrm{sw},2} \, \tau_{\mathrm{sw},2} + R_{\mathrm{on},2} \, \frac{P_{\mathrm{sc}}^2}{u_{\mathrm{sc}}^2}, \tag{3}$$

for the battery module

$$\ell_{\mathrm{bat}} = |P_{\mathrm{bat}}| \frac{u_{\mathrm{bus}}}{u_{\mathrm{bat}}} \, f_{\mathrm{sw},3} \, \tau_{\mathrm{sw},3} + R_{\mathrm{on},3} \, \frac{P_{\mathrm{bat}}^2}{u_{\mathrm{bat}}^2}, \tag{4}$$

the photovoltaic array module

$$\ell_{\mathrm{pv}} = |P_{\mathrm{pv}}| \frac{u_{\mathrm{bus}}}{u_{\mathrm{pv}}} \, f_{\mathrm{sw},4} \, \tau_{\mathrm{sw},4} + R_{\mathrm{on},4} \, \frac{P_{\mathrm{pv}}^2}{u_{\mathrm{pv}}^2}. \tag{5}$$

In these expressions, $f_{\mathrm{sw,j}}$ is the switching frequency of module $j$. $\tau_{\mathrm{sw,j}}$ is the switching time that lumps together switching on, switching off losses, including all switching phenomena. Conduction losses are mostly resistive as MOSFET devices are employed and as they are conducting actively in both directions (current in the diode is negligible). The difference between the forward and backward conduction of the MOSFET devices is neglected for simplicity.

(3)-(5) suggest that the smaller the bus voltage the smaller the losses, which justifies the bus voltage selection strategy of relation (1). Moreover, the losses increase as the accumulator and PV module voltages decrease. Not taking into account drive losses, this would suggests selecting voltages as high as possible. However, the drive losses need to be taken into account to design the voltage levels as they are linked to the voltage selection through relation (1).

### B. Drive module losses

The motors electromechanical power and gear losses are computed from the applied vehicle force $F$ and velocity $\dot{x}$:

$$P_{\mathrm{mech}} = F \, \dot{x}. \tag{6a}$$

The gear losses depend on the sign of the torque, i.e. on the sign of the mechanical power:

$$\ell_{\mathrm{gear}} = \begin{cases} \left(1 - \frac{1}{\eta_{\mathrm{gear}}}\right) \, P_{\mathrm{mech}}, & P_{\mathrm{mech}} > 0 \\ (1 - \eta_{\mathrm{gear}}) \, P_{\mathrm{mech}}, & P_{\mathrm{mech}} \leq 0 \end{cases} \tag{6b}$$

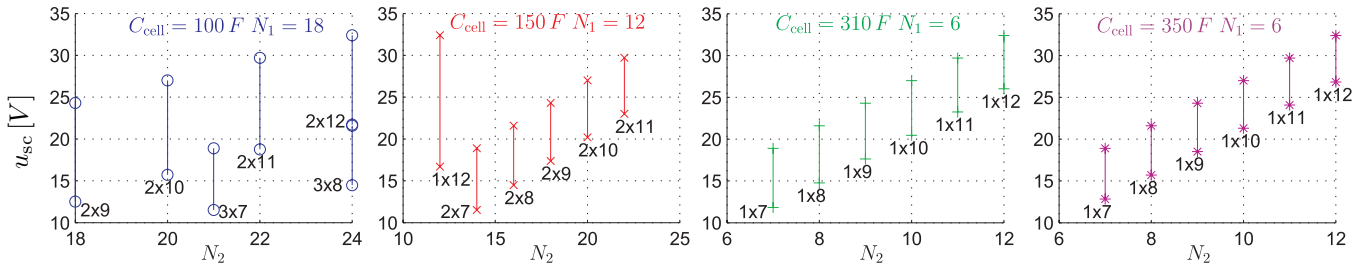


Fig. 5. Candidate supercapacitor arrangements after adding cells for compatibility with voltage requirements

Electromagnetic torque is obtained summing up (6a) and (6b):

$$P_{\text{em}} = P_{\text{mech}} - \ell_{\text{gear}} \tag{6c}$$

The effort is assumed to be balanced over the different motors, yielding equal motor currents, rotor velocities and required DC-voltage. Two non-salient permanent magnet synchronous motors (PMSM) are employed to drive the vehicle using field oriented control. For this type of PMSM and this type of control scheme, the torque is controlled through the quadrature axis $i_{s,q} = 0$ axis while $i_{s,d} = 0$ for most range of operation:

$$i_{s,q} = \frac{P_{\text{em}}}{2\,k_T\,\omega_r}. \tag{7a}$$

The angular velocity is linked to the vehicle speed through the gear ratio $\rho$, the number of pole pairs $p$ and the wheel radius $r_{\text{wheel}}$:

$$\omega_r = \frac{\dot{x}}{\rho\,p\,r_{\text{wheel}}}. \tag{7b}$$

The motor voltage is readily obtained from the torque constant $k_T$, stator inductance $L_s$ and resistance $R_s$:

$$u_{\text{mot}} = \sqrt{2\,\left[(k_T + L_s\,i_{s,q})\,\omega_r\right]^2 + 2\,\left[R_s\,i_{s,q}\right]^2} \tag{7c}$$

The motors' losses are obtained:

$$\ell_{\text{mot}} = 2\,R_s\,i_{s,q}^2 \tag{8a}$$

The drive losses are obtained summing up motor losses and drive power converters losses:

$$\ell_{\text{drive}} = 2\,u_{\text{bus}}\,i_{s,q}\,f_{\text{sw},1}\,\tau_{\text{sw},1} + 2\,R_{\text{on},1} i_{s,q}^2 \tag{8b}$$

The total power consumed by the drives, including the control, is obtained:

$$P_{\text{drive}} = P_{\text{mech}} + \ell_{\text{gear}} + \ell_{\text{mot}} + \ell_{\text{drive}} + \ell_{\text{con}} \tag{9}$$

where the DC bus voltage is given by relation (1).

### C. Overall losses

The overall losses are obtained summing (3)-(5) and (9). They depend on the voltage levels and on the driving profile which sets the power flows. The voltage levels depend on the nominal voltage and capacity that are selected at the design stage and on the control strategy. The selection of the optimal voltages should therefore be based on the driving profiles, which is the topic of section V.

## V. Optimal supercapacitor tank design for energy management loss minimization

In this section, the accumulator that features the best trade-off between minimum energy storage and minimum power losses is selected using the loss model derived in section IV among the candidate supercapacitor arrangements designed in section III. The driving and sun power probability distributions are used to determine the most likely case that is minimizing the vehicle power losses.

### A. Stochastic models of the power production and driving conditions

The photo-voltaic power production and driving conditions are the two stochastic inputs of the system. Two main approaches allow to model these stochastic inputs: a) probability distributions can be build using large amount of driving data or b) stochastic models can be build from a reduced amount of data combining different knowledge models. The second approach was taken in the present work to build a model of solar energy production and of driving conditions.

*1) Driving profile stochastic model:* Fig. 3 shows the deterministic worst case driving profile employed to determine the vehicle energy requirements. It is assumed the driving profile is piecewise affine. It is therefore made of segments of given length, slope and limited speed. The length of the segment and slope are continuous time stochastic variables. The slope of a segment is correlated to its length as steep segments tend to be shorter. The slope of a segment is moreover correlated to the past slope and lengths. The vehicle speed is linked to maximum admissible speed for a segment. Maximum admissible speed can take only discrete values. It is assumed that the maximum admissible speed is constant over a segment. The vehicle speed has a probability distribution around the maximum admissible speed: we use a Gaussian distribution for simplicity. The deviation to the maximum admissible speed is correlated to past deviation. The energy to change speed between the segments is considered but it is diluted over the segment for simplicity. This can be written as a Markov chain process:

$$\boldsymbol{x}_{k+1} = \boldsymbol{A}\,\boldsymbol{x}_k + \boldsymbol{\xi}_k \tag{10a}$$

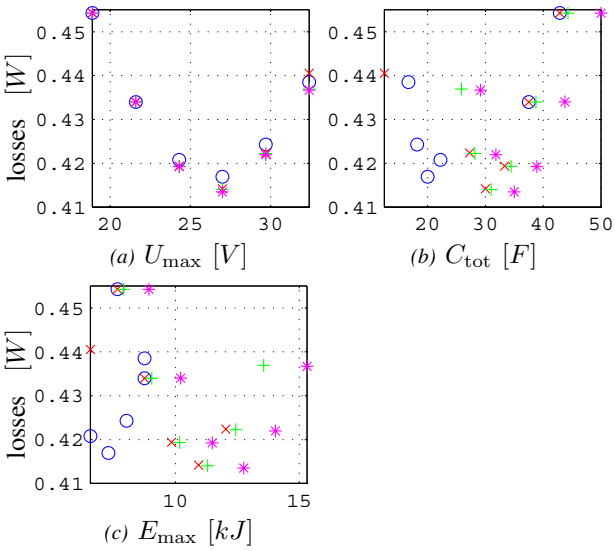


Fig. 6. Power losses along (a) supercapacitor tank maximum voltage axis, (b) supercapacitor tank capacity, (c) supercapacitor tank maximum energy.

where $\boldsymbol{\xi}_k$ is a noise; the state $\boldsymbol{x}_k$ is obtained taking realizations of the process over an horizon of influence:

$$\boldsymbol{x}_k = \begin{bmatrix} \boldsymbol{y}_k \\ \boldsymbol{y}_{k-1} \\ \vdots \\ \boldsymbol{y}_{k-N} \end{bmatrix} \qquad \boldsymbol{y}_k \equiv \begin{bmatrix} \text{length}(k) \\ \text{slope}(k) \end{bmatrix} \tag{10b}$$

where the current realization is obtained from the state at each sampling period:

$$\boldsymbol{y}_k = \boldsymbol{C}\, \boldsymbol{x}_k \tag{10c}$$

*2) Solar power profile stochastic model:* A similar process as in paragraph V-A1 is employed to model the sun power, which is constrained to be positive. Relatively sophisticated modeling approaches can be employed to predict seasonal effects and correlation [7]. To simplify our procedure and as the considered time horizon is relatively short, a time invariant probability distribution without past correlation is considered in this work.

### B. Simulation results

Employing the model of section IV, the losses are computed for the 24 candidate supercapacitor arrangements that have been designed in section III. It can be seen in Fig. 6(a) that the losses are mostly sensitive to the maximum voltage of the tank, which modifies the bus voltage distribution, which affects the losses as suggested in IV. Fig. 6(b) and (c) do not allow to deduce a direct relation between the tank capacity and the losses nor between the tank energy and the losses.

### C. Pareto minimum

The mass/volume/cost of the supercapacitor accumulator are associated to its maximum energy. The trade-off between minimum losses and minimum accumulator mass/volume/cost

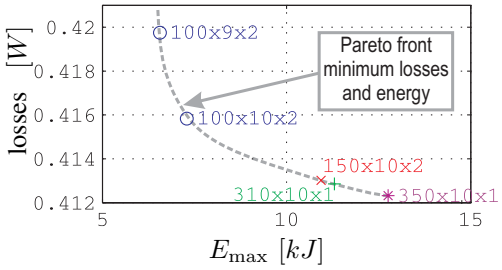


Fig. 7. Pareto front illustrates tradeoff between minimum losses and accumulator energy.

is captured by the Pareto front represented in Fig. 7. From this Pareto front, it can be deduced that the optimal arrangement of supercapacitors for the trade-off mass/volume/cost/losses is 100Fx10x2.

## VI. Conclusion

A design methodology has been proposed to minimize the required energy storage capacity of an hybrid accumulator and the associated system losses. A reduced scale solar electric vehicle is considered for illustration. Supercapacitor arrangements that fulfill power, energy and voltage constraints are designed based on a worst case driving scenario. The system losses are modeled analytically. Driving conditions and solar irradiance scenarios are obtained employing stochastic models. The losses associated losses mostly depend on the accumulator maximum admissible voltage and driving conditions. The Pareto front that captures the trade-off between accumulator minimum storage energy and vehicle minimum losses is obtained; the accumulator that features the best trade-off is selected.

## References

[1] A. Rufer and P. Barrade. A supercapacitor-based energy-storage system for elevators with soft commutated interface. *IEEE Trans. on Ind. Ap.*, 38(5):1151 – 1159, 2002.

[2] A. Allegre, A. Bouscayrol, P. Delarue, P. Barrade, E. Chattot, and S. El-Fassi. Energy storage system with supercapacitor for an innovative subway. *IEEE Trans. on Ind. El.*, forthcoming, 2010.

[3] A. Rufer, D. Hotellier, and P. Barrade. A supercapacitor-based energy storage substation for voltage compensation in weak transportation networks. *IEEE Trans. on Power Del.*, 19(2):629 – 636, 2004.

[4] W. Lhomme, P. Delarue, P. Barrade, P. Bouscayrol, and A. Rufer. Design and control of a supercapacitor storage system for traction applications. In *Proc. Ind. App. Conf.*, volume 3, pages 2013 – 2020, 2005.

[5] B. Destraz, P. Barrade, A. Rufer, and M. Klohr. Study and simulation of the energy balance of an urban transportation network. In *Proc. European Power El. Conf.*, pages 1 – 10, 2007.

[6] Bo Chen, Gao Yimin, M. Ehsani, and J.M. Miller. Design and control of a ultracapacitor boosted hybrid fuel cell vehicle. In *Proc. Veh. Power Prop. Conf.*, pages 696 – 703, 2009.

[7] T.L. A. Urbina and R.G. Jungst Paez. Stochastic modeling of rechargeable battery life in a photovoltaic power system. In *Energy Conversion Engineering Conf. and Exhibit*, volume 2, pages 995 –1003, 2000.

[8] L. Grigans and L. Latkovskis. Estimation of the power and energy requirements for trackside energy storage systems. In *European Power Electronics and Applications Conf.*, pages 1 –7, 8-10 2009.

[9] S. Mariéthoz. http://control.ee.ethz.ch/ cpes/ev/ev.php, 2008-2010.

[10] P. Barrade and A. Rufer. Current capability and power density of supercapacitors: considerations on energy efficiency. In *Proc. European Conf. on Power Electronics and Applications, EPE*, 2003.